

Spin control in semiconductor quantum wires: Rashba and Dresselhaus interaction

R. G. Nazmitdinov

Departament de Física, Universitat de les Illes Balears, E-07122 Palma de Mallorca, Spain and Bogoliubov Laboratory of Theoretical Physics, Joint Institute for Nuclear Research, 141980 Dubna, Russia

K. N. Pichugin

Kirensky Institute of Physics, Akademgorodok 50/38, 660036 Krasnoyarsk, Russia

M. Valín-Rodríguez

Conselleria d'Educació i Cultura, E-07004 Palma de Mallorca, Spain

(Received 1 April 2009; published 6 May 2009)

We show that spin precession in a semiconductor quantum wire, caused by the Rashba and the Dresselhaus interactions (both of arbitrary strengths), can be suppressed by dint of an in-plane magnetic field. Using a condition of the translational invariance in the longitudinal coordinate, we found another type of symmetry, which arises at a particular set of intensity and orientation of the magnetic field and explains this suppression. Based on our findings, we propose a transport experiment to measure the strengths of the Rashba and the Dresselhaus interactions.

DOI: [10.1103/PhysRevB.79.193303](https://doi.org/10.1103/PhysRevB.79.193303)

PACS number(s): 73.63.Nm, 72.25.Dc, 71.70.Ej, 85.75.-d

Spin-polarized transport in semiconductor nanostructures is the main topic in spintronics due to great interests to both basic research and device application.^{1,2} Spin-orbit interactions present in semiconductor structures provide a promising way to spin manipulation in bulk semiconductors,³ two-dimensional (2D) electron gases,⁴ and quantum dots.⁵ However, these interactions cause decay of spin polarization⁶ since the spin-orbit coupling breaks the total spin symmetry. The effect of spin relaxation produced by the interplay between the Dresselhaus⁷ and Rashba⁸ spin-orbit interactions (RDIs) has been studied in a few publications (cf. Refs. 9–14). It was found by Schliemann *et al.*¹⁰ that at zero magnetic field in 2D semiconductor nanostructures for equal strengths of the RDI there is an additional symmetry.¹⁴ As a consequence, the orbital motion is decoupled from the spin evolution. If this resonant condition is not active, the spin dynamics is influenced by the different spin relaxation mechanisms related to orbital scattering processes. In this Brief Report we discuss another spin symmetry that arises at certain conditions at nonzero magnetic field in the plane and arbitrary strengths of the spin-orbit terms in a quantum wire. In virtue of this symmetry the spin precession is suppressed at arbitrary polarization of the injected electrons. By setting these conditions “on” and “off,” the flow of a certain spin polarization through the device is either allowed or destroyed, thus, defining a transistorlike action for the spin.

We consider the conduction band of a 2D semiconductor quantum well within the effective mass approximation. The wire geometry is defined by a transversal potential $V(y)$: $\mathcal{H}_0 = (p_x^2 + p_y^2)/2m^* + V(y) = \mathcal{H}_y + p_x^2/2m^*$. The Dresselhaus interaction has, in general, a cubic dependence on the momentum of the carriers. For a narrow $[0,0,1]$ quantum well, it reduces to the 2D linear momentum dependent term $\mathcal{H}_D = \beta(p_x\sigma_x - p_y\sigma_y)/\hbar$ (β is the interaction strength). In the asymmetric quantum wells the Bychkov-Rashba interaction has the form $\mathcal{H}_R = \alpha(p_y\sigma_x - p_x\sigma_y)/\hbar$, where α is the corresponding strength. Our system Hamiltonian reads as

$$\mathcal{H} = \mathcal{H}_0 + \mathcal{H}_D + \mathcal{H}_R + \mathcal{H}_Z, \quad (1)$$

where we include the effect of the in-plane magnetic field by means of the Zeeman interaction $\mathcal{H}_Z = g^* \mu_B B (\cos \theta \sigma_x + \sin \theta \sigma_y)/2 = \varepsilon_z (\cos \theta \sigma_x + \sin \theta \sigma_y)/2$. Here, θ represents the in-plane orientation of the magnetic field with the intensity B , g^* is the effective gyromagnetic factor, and μ_B is the Bohr magneton.

Note that none of the interactions break the translational invariance in the longitudinal coordinate. Therefore, the eigenstates are chosen to have a well-defined longitudinal momentum $\hbar k$,

$$\Psi_{nks}(\vec{r}) = e^{ikx} \begin{pmatrix} \chi_{nks\uparrow}(y) \\ \chi_{nks\downarrow}(y) \end{pmatrix} =: e^{ikx} \chi_{nks}(y), \quad (2)$$

where n , k , and s stand for transversal, longitudinal, and spin quantum numbers. As a result, Hamiltonian (1) is transformed to the effective one for the transversal coordinate for a given value of k ,

$$\mathcal{H}_{\text{eff}} = \mathcal{H}_y + \frac{p_y}{\hbar} (\alpha \sigma_x - \beta \sigma_y) + \left[\left(\beta k + \frac{\varepsilon_z}{2} \cos \theta \right) \sigma_x - \left(\alpha k - \frac{\varepsilon_z}{2} \sin \theta \right) \sigma_y \right]. \quad (3)$$

Two different spin-dependent terms can be distinguished within this Hamiltonian: one involves the transversal component of the momentum and the other contains the effective Zeeman-type term including contributions from the RDI. If both terms are parallel in the spin space, a symmetry arises and the spin is totally decoupled from the orbital motion. In order to set this symmetry, it is required to fulfill the following condition:

$$\frac{2\alpha k_0}{\varepsilon_z} \left[1 - \left(\frac{\beta}{\alpha} \right)^2 \right] = \sin \theta + \frac{\beta}{\alpha} \cos \theta. \quad (4)$$

Once Eq. (4) is fulfilled, the spin operator $\mathcal{S}_{xy} = \alpha\sigma_x - \beta\sigma_y$ commutes with the resulting Hamiltonian,

$$\mathcal{H}_{\text{eff}} = \mathcal{H}_y + \left[\frac{p_y}{\hbar} + \frac{1}{\alpha}(\beta k_0 + \varepsilon_z \cos \theta/2) \right] (\alpha\sigma_x - \beta\sigma_y), \quad (5)$$

i.e., $[\mathcal{H}_{\text{eff}}, \mathcal{S}_{xy}] = 0$. Consequently, the spin symmetry is set up for transversal eigenstates having longitudinal momentum $k = k_0$. According to Eq. (4), this can be done by tuning a proper intensity ($\sim \varepsilon_z$) and an orientation of the applied in-plane magnetic field for given strengths α and β . It is noteworthy that this property is valid for any transversal potential defining the wire geometry since the symmetry arises from the relation between the RDI and the Zeeman interaction in conjunction with the longitudinal translational invariance. In addition, there is an extra degree of freedom since the RDI strengths (for example, α) can be modified as well in order to fulfill condition (4).

In virtue of the spin symmetry, the spinorial part of the eigenstates can be expressed as

$$\chi_s = \frac{1}{\sqrt{2}} \begin{pmatrix} 1 \\ s e^{-i\phi} \end{pmatrix}, \quad \phi = \arctan(\beta/\alpha), \quad (6)$$

where thereafter $s = \pm 1$. These eigenspinors correspond to the in-plane orientation of the spin, where the particular orientation is determined by the ratio between the strengths of both spin-orbit mechanisms. Note that in Hamiltonian (5) the spin-dependent term, linear in the transversal momentum p_y , can be eliminated by redefining the origin of the transversal momentum for each spin state. The only effect of this term on the energy spectrum is a constant shift that may be neglected by changing the energy's origin.

At condition (4) hold fixed, the spectrum of the system is composed of that corresponding to the spin-independent orbital motion $\mathcal{H}_0(\varepsilon_{nk}^0)$, the constant shift, and a contribution arising from a combination of the RDI strengths and the Zeeman interaction,

$$\varepsilon_{nk_0s} = \varepsilon_{nk_0}^0 - \frac{m^*}{2\hbar^2} r^2 + \frac{s}{\alpha} \left(\beta k_0 + \frac{\varepsilon_z}{2} \cos \theta \right) r. \quad (7)$$

Here we introduced the absolute magnitude of the RDI strength vector $r = \sqrt{\alpha^2 + \beta^2}$. The above contribution represents a constant spin splitting for the eigenstates and its value depends on the longitudinal momentum, the RDI strengths, the particular orientation, and the intensity of the applied magnetic field. At the preserved symmetry the eigenstates [Eq. (2)] take the form

$$\Phi_{nk_0s}(\vec{r}) = e^{-isy/\ell_{\text{RDI}}} e^{ik_0x} \psi_n^0(y) \chi_s, \quad (8)$$

where $\psi_n^0(y)$ are the eigenstates of \mathcal{H}_y . We have also defined the length $\ell_{\text{RDI}} = \hbar^2 / (m^* r)$ giving the characteristic scale for the RDI strengths.

At given Fermi energy E_F eigenstates [Eq. (2)] have a few real longitudinal momenta k . Some of them have $k > 0$

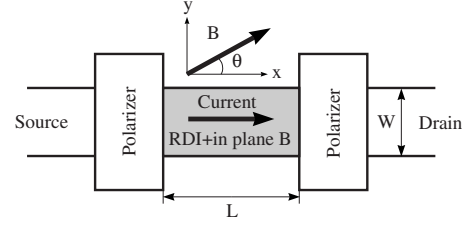


FIG. 1. Sketch of the 2D wire device.

(propagating right), while the others have $k < 0$ (propagating left). One of those k could satisfy condition (4) by the adjusted magnetic field and, consequently, the corresponding spinor does not depend on coordinates. However, even a small mixing between the selected state and those that propagate in the same direction but have different k leads to the spin precession in the process of the propagation. To suppress unwanted k values one can adjust the Fermi energy to have only four real longitudinal momenta. The same effect can be reached by altering the potential $V(y)$ since the influence of the lateral confinement on the RDI strengths is negligible.¹⁵ Next, the tuning of the intensity and the orientation of the magnetic field enables us to have two eigenstates [with $s = \pm$ in Eq. (7)], propagating in the same direction, with the same energy and k_0 . From Eqs. (4) and (7) one obtains that such a possibility can be realized if the components of the magnetic field are proportional to the components of the RDI vector,

$$\frac{\varepsilon_z}{2} \cos \theta_0 = -k_0 \beta, \quad \frac{\varepsilon_z}{2} \sin \theta_0 = k_0 \alpha. \quad (9)$$

As a result, there is no spin precession for any superposition of these eigenstates. Note that, in contrast to the spin-field transistor proposed in Ref. 10 whose effect is based on a particular input spin polarization, in our case the spin precession is absent for an arbitrary input spin polarization. Also, the magnetic field leads to a nonequivalence of the electron transport from the left to the right and vice versa: Eq. (9) is fulfilled for $-k_0$ at the condition $\theta_0 \rightarrow \theta_0 + \pi$.

To illuminate the found effect in the electron transport we perform numerical calculations of the S matrix in the tight-binding model (cf. Ref. 16). To proceed we use a square lattice $n = n_x \hat{x} + n_y \hat{y}$ (\hat{x} and \hat{y} are vectors of a length a_0 in x and y directions, respectively, a_0 is the lattice constant, and n_x and n_y are integers). For the sake of illustration, we choose for the wire potential a hard wall one: $V(y) = 0$ for $0 < y < W$ and $V(y) = \infty$ otherwise.

Let us consider the system with a geometry shown in Fig. 1. It consists of a finite scattering area with two lateral contacts. Each contact is a narrow stripe with the width $W = 20a_0$ and, for simplicity, no spin-orbit couplings and no the magnetic field. The contacts are gated to have two active channels (spin up and down) with a conductance e^2/h in each. Thus, the RDI and the in-plane magnetic field present only in the scattering area of the length L and the width W . The experiment may consist of injecting a current I through the left contact (source) to the wire and measuring the voltage drop V_R generated in the right contact (drain). According

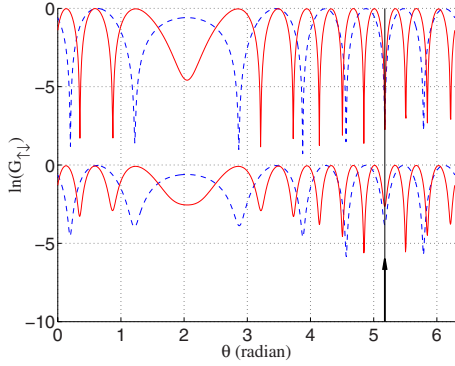


FIG. 2. (Color online) The logarithm of the spin-flip conductance (in units of e^2/h) as a function of the magnetic field orientation θ (the intensity $B=1.8$ T) for different sample lengths: $L=31W$ (solid line) and $L=17W$ (dashed line). Temperatures are $T=0$ K (top) and $T=1$ K (bottom). The incoming electrons are polarized along z axis. The set of parameters is typical for InAs: $E_F=10$ meV, $W=45$ nm, $\alpha=20$ meV nm, $\beta=10$ meV nm, $g^*=-14.9$, and $m^*=0.023m_e$. The arrow indicates the unique position of the angle θ_0 for non-spin-flip conductance, independent of the sample length.

to the Landauer-Buttiker formalism for linear response (cf. Ref. 17), the ratio V_R/I can be expressed by dint of the S -matrix elements $S_{m\sigma_2 n\sigma_1}$, where $n\sigma_1$ ($m\sigma_2$) denote the channels in the source (the drain). In our approach the spin resolved conductance between the source and the drain is determined as $G_{\sigma_1\sigma_2} = e^2/h \int dE [-f'(E-E_F)] \sum_{nm} |S_{m\sigma_2 n\sigma_1}|^2$, where $f=1/\{1+\exp[(E-E_F)/k_B T]\}$. The conductance is calculated with the energy dependent S matrix by direct solving the Schrödinger equation in a discretized space according to the method suggested in Ref. 18. Similar techniques has been used recently to study spin polarized transport in quantum wires due to the Rashba interaction.¹⁹

Note that the interfaces (the polarizers) between areas with and without the RDI introduce some uncontrollable excitations of all modes inside the scattering area. In particular, these excitations produce a superposition (with coefficients a_1 and a_2) of two eigenfunctions $\chi_{1,2}(y)\exp(ik_{1,2}x)$ with different longitudinal momenta and, therefore, rotate the spin during a transport along the x axis. Indeed, one has the following expectation values: $\langle S_x \rangle = \text{Re } \xi$, $\langle S_y \rangle = \text{Im } \xi$, where $\xi = (a_1^* \chi_{1\uparrow}^* + a_2^* \chi_{2\uparrow}^*)(a_1 \chi_{1\downarrow} + a_2 \chi_{2\downarrow}) \exp[i(k_2 - k_1)x]$. Evidently, for equal longitudinal momenta, the expectation values are independent of the x coordinate. The results (see Fig. 2, top) manifest a single common minimum of the spin-flip conductance ($\sim 10^{-3}e^2/h$) for one value of the magnetic field orientation but for different sample lengths at a given intensity of the magnetic field and at zero temperature. At this value Eq. (9) holds, indeed. For another angles there is the mixing of wave functions with different k which leads to the electron spin rotation in the sample. Figure 3 illuminates the dependence of longitudinal momenta $k(\theta)$ on the magnetic field orientation. At a particular value of the angle θ_0 two wave numbers coincide. However, the change in the magnetic field intensity (the value of ε_z) leads to avoided crossing of two curves $k(\theta)$.

In order to assess possible limitations of the model, let us

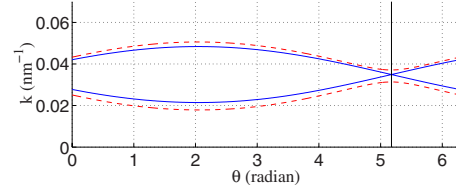


FIG. 3. (Color online) The longitudinal momentum k as a function of the orientation of the magnetic field (the angle θ) which intensity is subject to Eq. (9) (solid line) and is slightly different (dashed line). At the value $\theta_0=5.176$ (vertical line) both positive k 's coincide. The parameters are the same as for Fig. 2.

discuss a few mechanisms that may obscure the found effect for the ballistic transport. In real experiments the injected beam consists of electrons with different energies due to, for example, a nonzero temperature. The temperature induces a small mixture of spin-flip components and results in the increase in the spin-flip conductance (see Fig. 2, bottom). However, it does not affect the angle value at which the minima occur simultaneously in the two samples at temperature $T=1$ K.

The Zeeman interaction induces the orbital degrees of freedom in the vertical direction. Note, however, that in 2D systems, the orbital effect of the applied in-plane magnetic field is frozen due to the strong confinement in the vertical direction produced by the electrostatic potential of quantum well. Indeed, the magnetic parabola associated with the applied field introduces a negligible correction to the quantum well's potential. For example, for a typical well thickness (e.g., $z \approx 10$ nm) the applied magnetic field creates a magnetic potential $V_z = m^* \omega_c^2 z^2 / 2 \approx 0.0088 m_e / m^* [B]^2$ meV. The effective vertical potential V_z introduces a correction of $\sim 0.0005(\text{GaAs}) - 0.002(\text{InAs})$ eV at the magnetic field intensities up to 2 T, while the built-in electrostatic quantum well's potential has a characteristic energy scale of 0.2–0.4 eV. To reduce the effect of the magnetic parabola we require that $z < \ell_B$ ($\ell_B = \sqrt{\hbar c / eB}$ is the magnetic length).

The width W should be evidently larger than the thickness

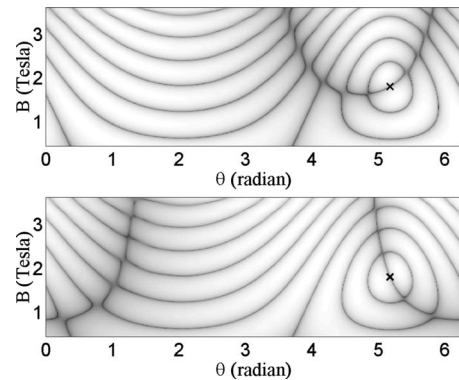


FIG. 4. The logarithm of the spin-flip conductance (in units of e^2/h) as a function of the intensity B and orientation θ of the magnetic field for the sample length $L=31W$ and temperature $T=0$ K (the darker the line is, the lesser the conductance is). The input polarization is along x axis (top) and y axis (bottom). The minimum due to Eq. (9) is pointed by \times mark. The parameters are the same as for Fig. 2.

but should be smaller than the ℓ_{RDI} (to diminish backscattering from the wire interfaces): $W \ll \ell_{\text{RDI}}$. The Fermi energy and the transversal potential $V(y)$ should be taken to support only four propagating modes (two right moving and two left moving). Assuming that Eq. (9) is fulfilled, one obtains a useful estimation for the intensity $B \leq 2\sqrt{3}\pi r / (g^* \mu_B W)$ with the aid of the hard wall potential. The combination of the above two conditions gives $W \ll [(2\sqrt{3}\pi \hbar^2) / (m^* g^* \mu_B B)]^{1/2}$.

Measurement of the RDI strengths is a subject of intensive experimental efforts.^{4,20} We recall that Eq. (9) enables us to determine the strengths of the Rashba and Dresselhaus interactions. We propose to use a wire with a length determined by the condition $kL / (2\pi) \sim 5$. According to our analysis (see Fig. 4), such a system produces a few well resolved spin-flip conductance minima. This condition helps us also to diminish the effect of evanescent modes. The measurement of the spin-flip conductance provides a set of spin-flip minima at different intensities and different orientations of the magnetic field at a fixed input polarization. Taking another polarization and repeating the same measurement, one obtains a different pattern for the location of the minima. As an example, we calculate the spin-flip conductance for two input polarizations—along x and y axes (see Fig. 4). One obtains the required minimum which is subject to Eq. (9) at the same angle and the same intensity in different setups

since the effect is independent of the polarization. One might repeat measurements for different sample lengths since the minimum position is independent of the length too. To diminish the effect of multiple reflection from the polarizers we suggest to use the same polarization direction in both polarizers.

In conclusion, we found the condition [Eq. (4)] to decouple the spin and the orbital motion of electrons in a quantum wire with the in-plane magnetic field and arbitrary Rashba and Dresselhaus strengths. In virtue of the preserved longitudinal translational invariance and Eq. (4) there is the spin symmetry in an arbitrary transversal potential defining the wire geometry. At specific condition (9) the magnetic field cancels the RDI for the electron momentum k_0 . As a result, during the electron transport through the wire the spin precession is absent for any chosen polarization. We propose to measure the Rashba and the Dresselhaus interaction strengths by finding the minimum of the spin-flip conductance, which should occur at condition (9).

This work was partly supported by Ministerio de Ciencia e Innovacion (Spain), Grant No. FIS2008-00781/FIS and RFBR under Grants No. 08-02-00118 and No. 09-02-98005 (Russia).

¹I. Zutic, J. Fabian, and S. Das Sarma, *Rev. Mod. Phys.* **76**, 323 (2004).

²D. D. Awschalom and M. E. Flatté, *Nat. Phys.* **3**, 153 (2007).

³Y. Kato, R. C. Myers, A. C. Gossard, and D. D. Awschalom, *Nature (London)* **427**, 50 (2004).

⁴L. Meier, G. Salis, I. Shorubalko, E. Gini, S. Schön, and K. Enslin, *Nat. Phys.* **3**, 650 (2007).

⁵K. C. Nowack, F. H. L. Koppens, Y. V. Nazarov, and L. M. K. Vandersypen, *Science* **318**, 1430 (2007).

⁶M. I. D'yakonov, V. A. Marushchak, V. I. Perel', and A. N. Titkov, *Sov. Phys. JETP* **63**, 655 (1986).

⁷G. Dresselhaus, *Phys. Rev.* **100**, 580 (1955).

⁸Y. A. Bychkov and E. I. Rashba, *J. Phys. C* **17**, 6039 (1984).

⁹N. S. Averkiev, L. E. Golub, and M. Willander, *J. Phys.: Condens. Matter* **14**, R271 (2002).

¹⁰J. Schliemann, J. C. Egues, and D. Loss, *Phys. Rev. Lett.* **90**, 146801 (2003).

¹¹J. Kainz, U. Rössler, and R. Winkler, *Phys. Rev. B* **68**, 075322

(2003).

¹²M. Duckheim and D. Loss, *Phys. Rev. B* **75**, 201305(R) (2007).

¹³M. Ohno and K. Yoh, *Phys. Rev. B* **77**, 045323 (2008).

¹⁴B. A. Bernevig, J. Orenstein, and S.-C. Zhang, *Phys. Rev. Lett.* **97**, 236601 (2006).

¹⁵V. A. Guzenko, J. Knobbe, H. Hardtdegen, and Th. Schäpers, *Appl. Phys. Lett.* **88**, 032102 (2006).

¹⁶D. K. Ferry and S. M. Goodnick, *Transport in Nanostructures* (Cambridge University Press, New York, 1997).

¹⁷Y. Alhassid, *Rev. Mod. Phys.* **72**, 895 (2000).

¹⁸T. Ando, *Phys. Rev. B* **44**, 8017 (1991).

¹⁹A. W. Cummings, R. Akis, D. K. Ferry, J. Jacob, T. Matsuyama, U. Merkt, and G. Meier, *J. Appl. Phys.* **104**, 066106 (2008).

²⁰S. D. Ganichev, V. V. Bel'kov, L. E. Golub, E. L. Ivchenko, P. Schneider, S. Giglberger, J. Eroms, J. De Boeck, G. Borghs, W. Wegscheider, D. Weiss, and W. Prettl, *Phys. Rev. Lett.* **92**, 256601 (2004).